LSTM Controllers for Power Quality Improvement in Grid Connected Hybrid Wind-PV-Battery based Power Supply System

Ajay Agrawal, Neeraj Das, Sandeep Kumar Jain, and Kuldeep Singh Kulhar

Mr. Ajay Agrawal, Assistant Professor, Department of Mechanical Engineering, Sanskriti University, Mathura, Uttar Pradesh, India, Email Id- ajayagrawal.me@sanskriti.edu.in
Neeraj Das, Assistant Professor, Maharishi School of Engineering & Technology, Maharishi University of Information Technology, Uttar Pradesh, India, Email Id-dasium3000@gmail.com
Sandeep Kumar Jain, Assistant Professor, Electrical Engineering, Vivekananda Global University, Jaipur, India, Email Id-sandeep_jain@vgu.ac.in
Kuldeep Singh Kulhar, Professor, Civil Engineering, Vivekananda Global University, Jaipur, India, Email Id-k.singh@vgu.ac.in

Abstract— Nowadays, the popularity of grid integrated systems primarily supplied by renewable energy sources based hybrid Microgrids have increased. This is due to their ability to reduce global warming and meet the increasing electrical load demand worldwide. In order to guarantee an uninterrupted power supply to loads when operating in the operation of off-grid, the system incorporates a storage device, thereby establishing an effective energy management system. A new energy management system has been developed to enhance the stability of the proposed system. The system has the ability to stabilize voltage at the load bus, compensate for reactive power, and mitigate the harmonics as well as the effect of unbalanced load. In order to attain quick reactions amidst swift alterations, the suggested control technique has integrated LSTM controllers. Practical outcomes have been achieved by leveraging Hardware-in-the-Loop using OPAL-RT modules. Numerous case studies have been carried out to further confirm the efficacy of the suggested approach.

Keywords—Renewable Energy Sources, PV, Wind, LSTM, MPPT, Grid connected system.

Corresponding Author: ajayagrawal.me@sanskriti.edu.in

1. INTRODUCTION

The worldwide utilization of grid integrated renewable energy sources is steadily on the rise. Different systems, mainly relying on renewable energy sources, are being set up in small-scale industries, colleges, institutions, rooftops, and irrigation facilities to decrease pollution and supply electricity to local loads [1-4]. Additionally, PV-wind powered systems are readily available and easy to install, making them a popular choice for residential, commercial, and industrial applications. Nevertheless, the presence of both solar radiation and wind speed relies on atmospheric conditions [2-6]. Furthermore, the system is subject to sudden fluctuations in load that are beyond our control. Hence, incorporating a storage device is essential for preserving power equilibrium within the system. Although the grid plays a crucial role in balancing the power between the load and total generation in a Microgrid, it cannot ensure uninterrupted grid availability at all times. Hence, it is essential to incorporate a battery bank in such systems, especially in off-grid mode.

A common energy storage device used in Microgrids is a battery bank, which is made up of a combination of rechargeable batteries connected in series and parallel. Ensuring a consistent power supply to the load bus for 24 hours is a significant obstacle faced by grid-connected Microgrids, particularly when operating in off-grid operation. The objective of this research is to improve the cost-effectiveness of the system and elevate the power quality in grid integrated Microgrids.

In order to optimize the power output of photovoltaic (PV) and wind turbine systems, it is necessary to utilize devices like maximum power point tracking (MPPT) circuits. This is because the curves of these systems exhibit nonlinear characteristics, making it essential to employ MPPT circuits for achieving maximum power extraction. Several researchers have applied different MPPT methods to respective circuits [3-7]. Different circuits will be employed to create a strong DC-link that combines all power sources, such as batteries. An apparatus that allows for bidirectional power flow, with the ability to convert DC to DC, may be utilized for controlling the voltage of the DC-link. Furthermore, the system must include an inverter to provide AC power to the utility grid.

The loads within the power supply system will be managed at the point of common coupling (PCC). The loads are a combination of single-phase and three-phase components, potentially causing an imbalance in the line currents. This results in substandard power quality and gives rise to various problems throughout the grid. Hence, it is imperative to implement a new control technique in order to manage the inverter and address the aforementioned challenges in grid-connected systems.

Numerous academics have already utilized comparable systems employing varying control techniques. Nevertheless, the suggested control technique is designed to tackle supplementary concerns and improve power efficiency. Many researchers have employed proportional and integral (PI) controllers in their control models. Nevertheless, the LSTM-based control technique has shown superior performance compared to generalized PI controllers [6, 9].

2. DESCRIPTION OF THE SYSTEM

Figure 1 depicts the general system diagram of a grid-connected PV-battery-wind system. PMSG coupled wind turbines are primarily utilized in moderate power applications, in contrast to DFIG. A diode rectifier is required to convert the AC output power generated by the PMSG. Furthermore, the PMSG incorporates a boost device that operates as an MPPT circuit. A bidirectional circuit is situated between the battery bank and the dc-link. The DC

to DC circuit's control method is specifically engineered to function as an MPPT device for the PV system, thereby eliminating the necessity for extra converters. An inverter is necessary to provide alternating current (AC) electricity to the utility grid by regulating the voltage at the DC-link. In this research, a new control technique for the inverter has been introduced to improve power quality across different operational scenarios. The proposed inverter control utilizes LSTM controllers.

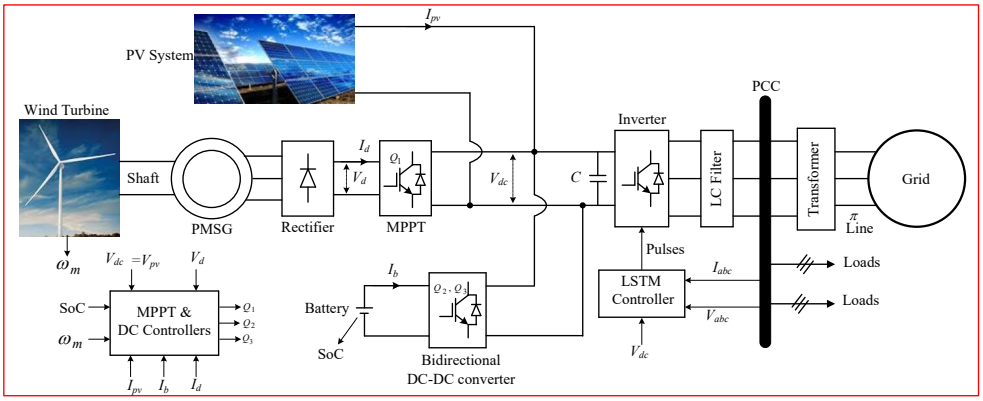

Fig. 1: Grid integrated hybrid system.

A research paper presents a new algorithm that effectively manages data from the smart grid by utilizing artificial neural networks (ANN) and long short-term memory (LSTM). The utilization of the LSTM algorithm boosts the functionalities of the ANN controller, whereas a deep learning algorithm is utilized to consistently modify the weights of the controller, facilitating adaptive learning and enhancing performance. Memory cells have been integrated into the design of the ANN-based controller unit, as depicted in Figure 2, in order to reduce the effects of noise signals within the smart grid. The fundamental equations are utilized to establish an LSTM block set, while Figure 3 illustrates its corresponding layout. Moreover, the system incorporates a machine learning algorithm to streamline the adaptation of neuron weights according to specific criteria. Moreover, the presence of unknown noise signals (ns) is taken into consideration during the analysis, as these signals may arise from high voltage and other components in the smart grid. In order to efficiently suppress these signals, the LSTM block takes into account the opposite polarity for each element.

$$a_t = \sigma(b_a + h_{t-1} \times w_{ah} + X_t \times w_{ax} \mp n_{sa}) \quad (1)$$

$$f_t = \sigma(b_f + h_{t-1} \times w_{fh} + X_t \times w_{fx} \mp n_{sf}) \quad (2)$$

$$\hat{C}_t = \tanh(b_c + h_{t-1} \times w_{ch} + X_t \times w_{cx} \mp n_{sc}) \quad (3)$$

$$O_t = \sigma(b_o + h_{t-1} \times w_{oh} + X_t \times w_{ox} \mp n_{so}) \quad (4)$$

$$s_t = f_t \otimes s_{t-1} + \hat{C}_t \times a_t \quad (5)$$

$$h_t = \tanh(s_t) \otimes O_t \quad (6)$$

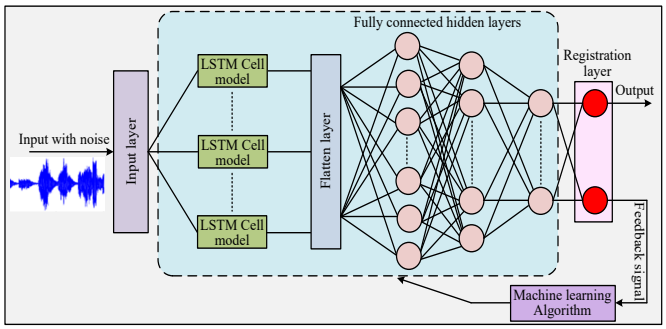

Fig. 2: ANN-LSTM model.

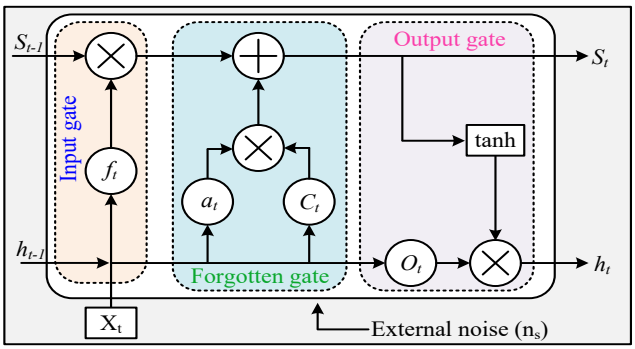

Fig. 3: a LSTM cell.

3. CONTROL METHODOLOGY OF INVERTER

The charging of the battery from renewable energy sources is given priority by the system. The battery bank's control enables charging when there is excess generation compared to the load. Additionally, the battery can discharge power into the load. Nevertheless, in the event that the battery reaches its maximum current or reaches full capacity, any excess power will be sent to the utility grid. Hence, the design of the inverter control takes into consideration the voltage at the dc-link. The LSTM model calculates the reference current of the active component (i_d^*) by analyzing the voltage at the dc-link in comparison to a reference value. This facilitates the smooth transfer of real power from the dc-link to the utility grid. The reference reactive current component (i_q^*) is derived by comparing the RMS voltage with its desired value in a similar manner. LSTM controllers are utilized to produce appropriate reference signals, guaranteeing accurate and smooth reactions. The reference signals are subsequently compared to the actual currents (i.e., i_d & i_q) in order to produce reference voltage signals. The inverter control incorporates decoupling components (ωLi_{dh} and ωLi_{qh}) and voltage components (v_d and v_q) to accommodate oscillations and harmonics. Figure 4 illustrates a block diagram of the inverter control. The suggested regulation of the inverter can function as an unbalanced compensation, guaranteeing equilibrium in the supply currents for the grid. This enables the supply of stable voltage to additional loads. The DC components of the reference voltage are converted into three-phase reference voltages.

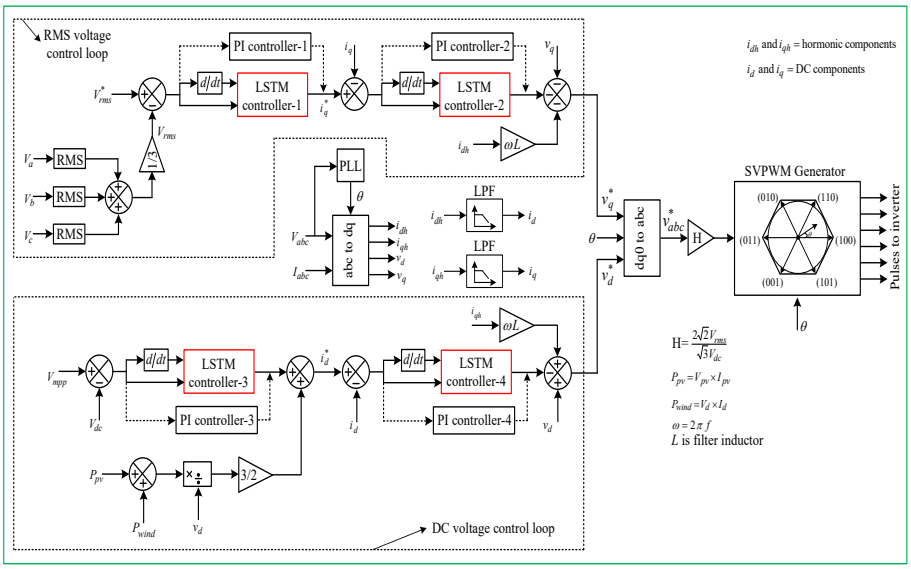

Fig. 4: Proposed control methodology of an inverter.

4. RESULTS AND ANALYSIS

The HIL has been established by utilizing OPAL-RT devices [10-12] to demonstrate varied responses across numerous case studies.

The utilization of real-time simulators (RTS) in this study enhances the performance of the system in various scenarios. To establish a hardware-in-the-loop (HIL) setup in the laboratory, the RTS units, specifically OPAL-RT units, are employed. Two OPAL-RT units are utilized to create the HIL environment for real-time testing of complex controllers. Within the OPAL-RT unit 1, the simulation involves the plant components such as PMSG, Converters, PV, Wind system, Grid, and others. However, OPAL-RT unit 2 is where all the controllers are implemented. The plant's analog signals undergo conversion into digital signals, which then function as inputs for the controller unit via data cards. The controller module functions according to the specified controllers and produces appropriate switching signals for the converters utilized within the facility. These digital pulses are then converted back to analog signals and serve as input signals for the plant through external data cards. Instead of utilizing an oscilloscope, a laptop is employed to present the results, providing improved visualization. Figure 5 illustrates the HIL setup, which consists of two OPAL-RT devices. The PV, battery, wind turbine, and other components' parameters in the DC Microgrid were sourced from references [13-17].

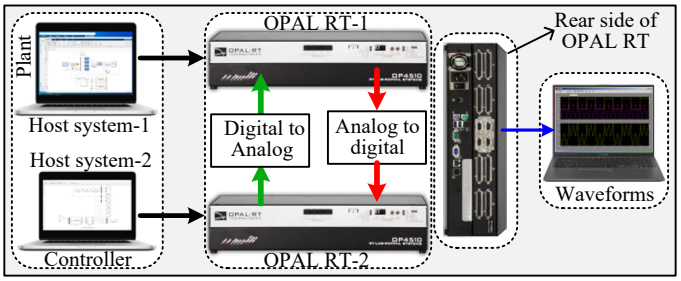

Fig. 5: HIL implementation.

Case-1: Changes in the system:

The analysis focused on the load consumption, irradiation, wind speed, etc. In order to obtain accurate results, a 15-hour time period was taken into consideration for all potential time conditions. Specifically, the time frame considered was from 7 AM to 10 PM. During the early morning and late evening, the sun irradiation tends to be low. The lowest irradiance occurs during the night, while it reaches its peak around midday. The changes in solar irradiance and wind speeds are depicted in Figure 6. According to Figure 6, the time scaling factor begins at 0 seconds, corresponding to 7 AM, and ends at 15 seconds, corresponding to 10 PM. The sun's irradiance peaks at 1000 w/m2 between 5 and 7 seconds. Similarly, the wind speed reaches its nominal value after 11 seconds, or 6 PM. Figure 7 provides a visual representation of the grid, battery, PV, and wind powers associated with these conditions.

The data was obtained during a steady state condition in order to enhance understanding. As a result, the starting time of Figure 9 does not begin at 0 seconds. By adjusting the upper limit of the limiter in Figure 3, it is assumed that the battery's initial State of Charge (SoC) is zero and its capacity fluctuates by 3 kW. Consequently, the battery can draw a maximum of 3 kW from the excess power generated, while the remaining energy is supplied to the grid. It is important to emphasize that the battery cannot be charged using grid power. Thus, the grid has the capability to solely consume energy and lacks the ability to generate power for battery charging. In Figure 9, this condition is depicted between 6 and 8 seconds, as well as 10 and 14 seconds. Any surplus power exceeding 3 kW is considered to be transferred to the utility grid.

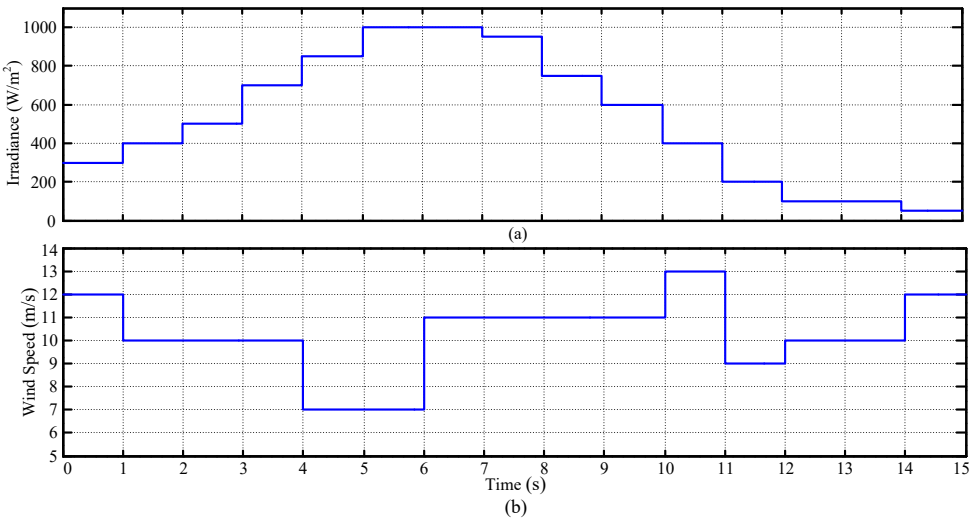

Fig. 6: Changes in (a) irradiance, (b) wind speed.

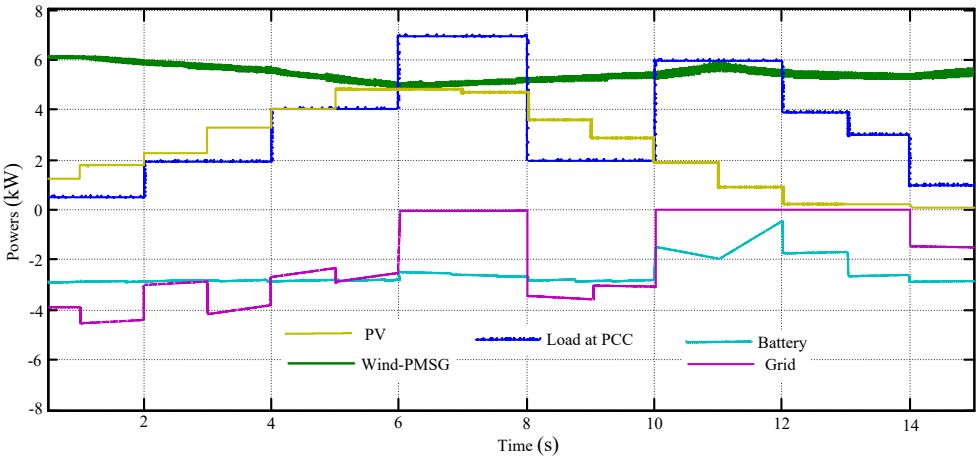

Fig. 7: Various powers.

Case-2: Operation under unbalanced load:

The PCC is currently facing an uneven distribution of load across its three phases, leading to a disruption in the grid voltages at the PCC. As depicted in Figure 6, the inverter has the ability to accommodate imbalanced current components. Consequently, the control mechanism of the inverter compels it to generate counterbalancing unbalanced currents. This, in turn, aids in balancing the grid currents when an unbalanced load is connected to the PCC. Consequently, the grid voltages are balanced as a result of the even droop across the transmission lines. Figure 8 showcases the unbalanced load connected to the PCC, while Figure 9 exhibits the corresponding balanced grid currents. Furthermore, the inverter is able to produce different modulation indices in order to maintain balanced PCC voltages. Figures 10 and 11 illustrate the instantaneous and RMS voltage waveforms respectively. In this particular situation, the imbalanced load is being utilized at the PCC for a period of 1.0 seconds.

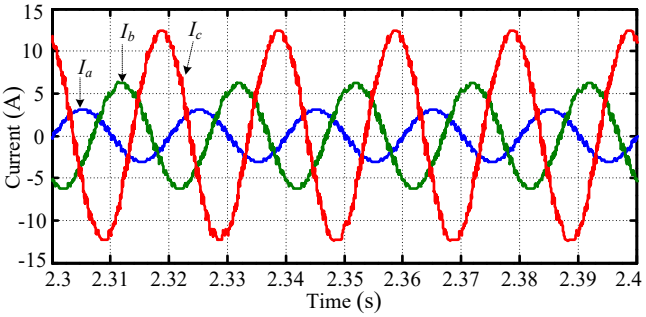

Fig. 8: Unbalanced currents.

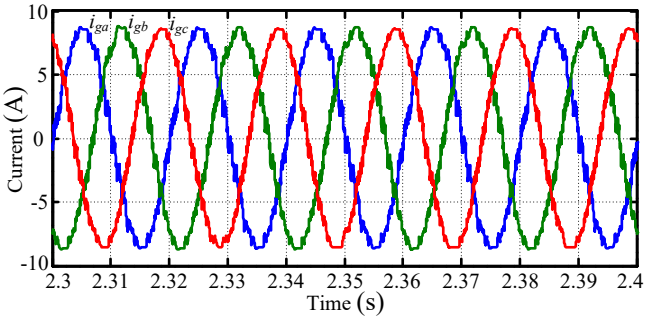

Fig. 9: balanced currents.

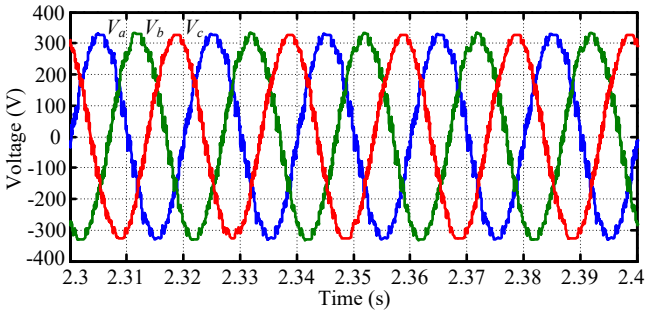

Fig. 10: Balanced 3-ph voltage.

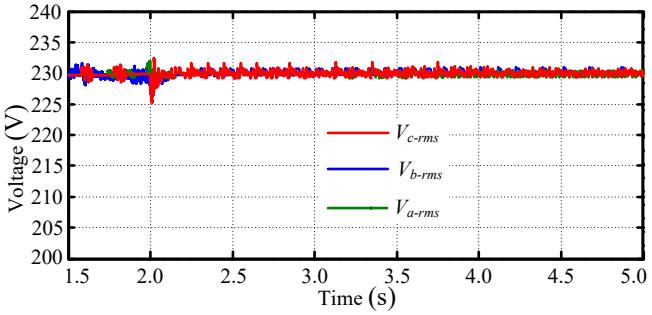

Fig. 11: 3-ph RMS voltage.

Case-3: During standalone operation:
The main focus of this study is on a grid-connected system that has the potential to transform into an isolated or standalone system when islanding occurs. When the system is disconnected from the grid, it operates independently with the battery managing the power. At t=2 seconds, an islanding condition arises due to an unbalanced load at the PCC. Additionally, the power generated by wind and PV sources falls short of the electricity consumed by the load. In this specific situation, because the grid is not linked to the PCC, it cannot provide power, thus relying solely on the battery for power management. Figure 12 (a) visually represents the different power levels. Following the islanding condition at t=2 seconds, the battery takes charge of fulfilling the power demand of the load. Figure 12 (b) displays the state of charge (SoC) of the battery. The accomplishment is achieved by maintaining the reference value of the dc-link voltage, as depicted in Figure 12(c). As stated earlier, an uneven distribution of load requires the inverter controller to produce

different modulation indices. This is done to ensure balanced RMS voltages at the PCC, as shown in Figures 12(d) and (e).

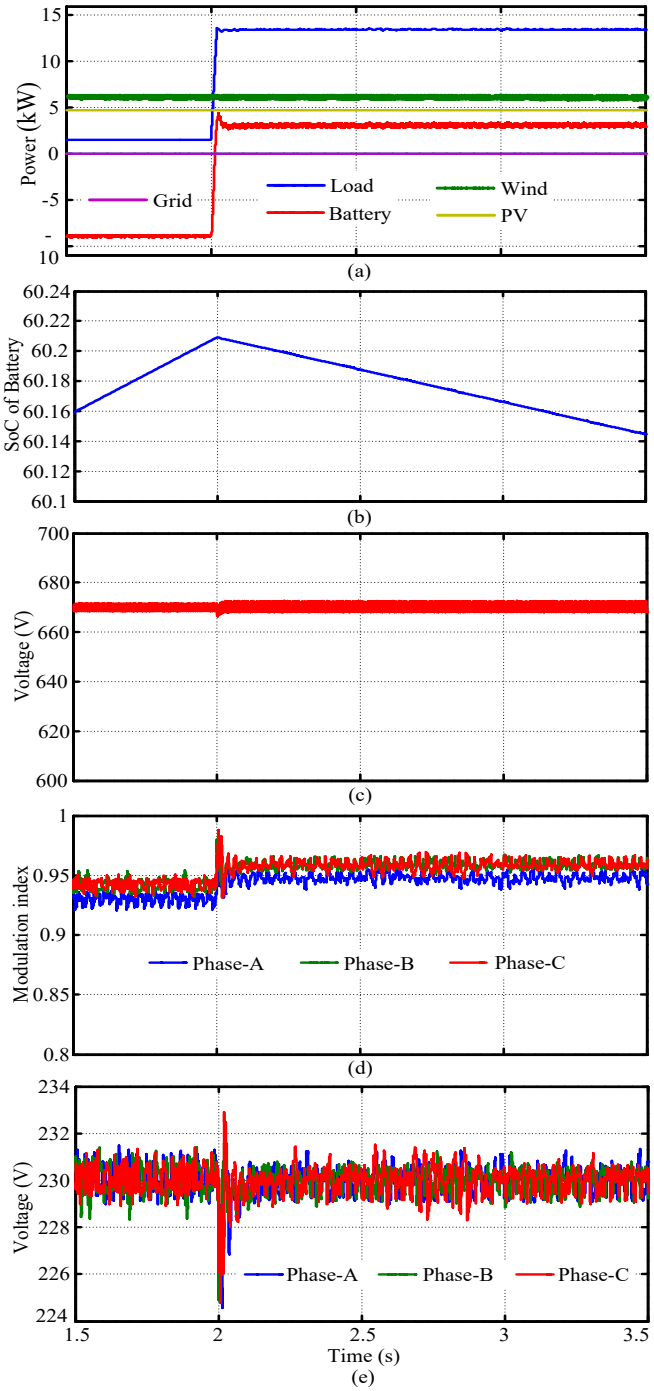

Fig. 12: under islanding operation (a) Powers, (b) SoC, (c) Voltage, (d) Modulation indexes, (e) 3-ph RMS voltage.

Case-4: Battery Responses.
The crafted ode underwent testing to assess the battery's performance under abrupt system modifications. Figure 13 illustrates the Power diagram associated with this evaluation, while Figure 14 depicts the Battery dc-link voltage. Furthermore, Figure 15 offers insights into the SoC of the battery, and Figure 16 showcases the instantaneous voltages at the load bus.

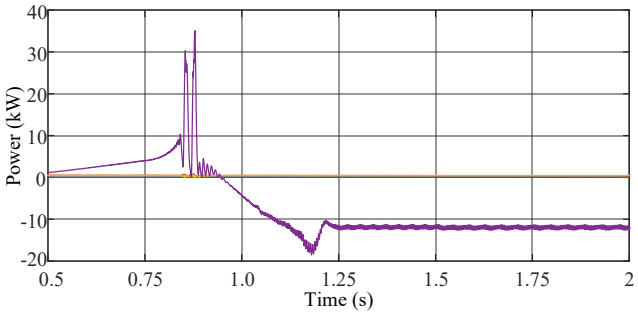

Fig. 13: Various powers.

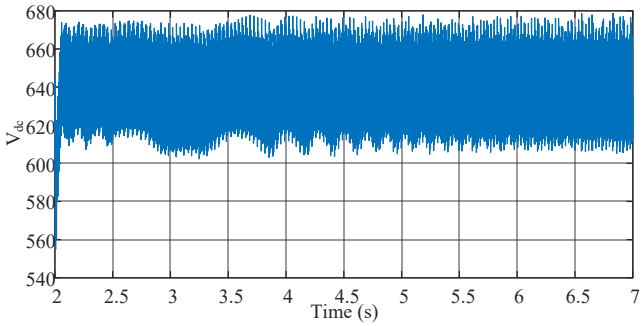

Fig. 14: Voltage at dc-link.

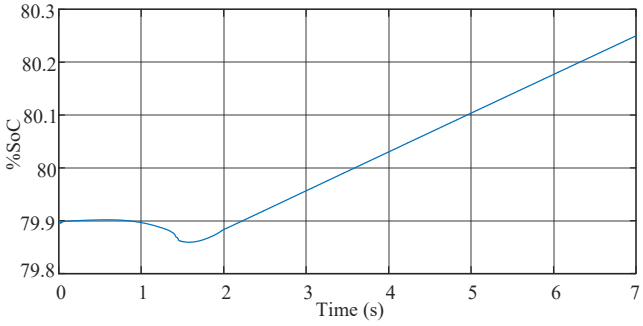

Fig. 15: SoC of the battery.

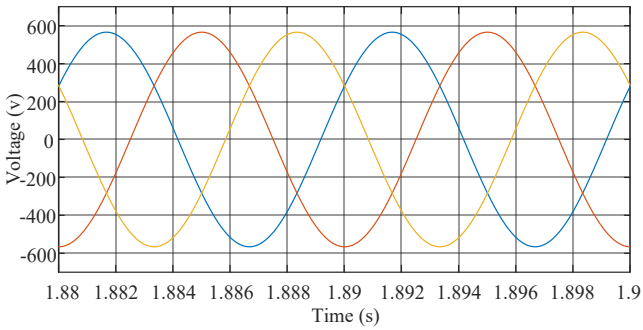

Fig. 16: Instantaneous 3ph voltage.

5. CONCLUSION

This research introduces LSTM-based regulators that are specifically designed for hybrid systems combining grid-connected PV and wind power. The main aim of the inverter controller is to enhance the quality of power. The research extensively focuses on component modeling and analysis. To optimize the power generation of a PV system, there is no need for an additional converter since the MPPT control and its algorithms are integrated within the DC-DC circuit. Several case studies are carried out to assess the efficiency of the suggested controllers.

References:

[1]. Müller S., Deicke M., and De Doncker Rik W. "Doubly fed induction generator system for wind turbines", *IEEE Industry Applications Magazine*, May/June, 2002, pp. 26-33.

[2]. M. E. Haque, K. M. Muttaqi, and M. Negnevitsky, "Control of a standalone variable speed wind turbine with a permanent magnet synchronous generator," in *Proc. IEEE Power and Energy Society General Meeting*, Jul. 2008, pp. 20–24.

[3]. M. E. Haque, M. Negnevitsky, and K. M. Muttaqi, "A novel control strategy for a variable-speed wind turbine with a permanent-magnet synchronous generator," *IEEE Trans. Ind. Appl.*, vol. 46, no. 1, pp. 331–339, Jan./Feb. 2010.

[4]. C. N. Bhende, S. Mishra and S. G. Malla, "Permanent Magnet Synchronous Generator based Stand-Alone Wind Energy Supply System", *IEEE Transactions on Sustainable Energy,* Vol. 2, No. 4, pp. 361- 373, Oct. 2011.

[5]. S. G. Malla and C. N. Bhende, "Voltage Control of Stand-Alone Wind and Solar Energy System", *Electrical Power and Energy Systems*, Vol. 56, pp. 361–373, March 2014.

[6]. S. G. Malla and C. N. Bhende, "Study of Stand-Alone Microgrid under Condition of Faults on Distribution Line", *International Journal of Emerging Electric Power Systems*, Issue 5, Vol. 15, 2014.

[7]. S. G. Malla, et al., "Wind and Photovoltaic based Hybrid Stand-Alone Power Generation System", *IEEE: International Conference on Energy, Communication, Data Analytics and Soft Computing (ICECDS 2017),*Chennai, India, 2017.

[8]. S. G. Malla, C. N. Bhende and A. Kalam, "Mitigation of Power Quality Problems in Grid-Interactive Distributed Generation System", *International Journal of Emerging Electric Power Systems*, Vol. 17, Issue 2, pp. 165-172, 2016.

[9]. S. G. Malla and C. N. Bhende, “Enhanced operation of stand-alone 'Photovoltaic-Diesel Generator-Battery' system”, *Electric Power System Research (Elsevier)*, Vol. 107, pp. 250-257, Feb. 2014.

[10]. P. A. Dahono and A. Purwadi, Qamaruzzaman, “An LC filter design method for single-phase PWM inverters,” in *Proc. Int. Conf. Power Electronics and Drive Systems*, 1995, vol. 2, pp. 571–576.

[11]. S. G. Malla et al., “SVM-DTC Permanent Magnet Synchronous Motor Driven Electric Vehicle with Bidirectional Converter”, *Automation, Computing, Communication, Control and Compressed Sensing, IEEE Xplore, 2013.*

[12]. Bose B.K, Power Electronics and Motor Drives, Academic Press, Imprint of Elsevier, 2006.

[13]. E. Muljadi, S. Drouilhet, R. Holz, and V. Gevorgian, “Analysis of permanent magnet generator for wind power battery charging,” in *Proc. IEEE Industry Applications Society Annual Meeting*, 1996, pp. 541–548.

[14]. A.M. Cross, P.D. Evans, and A. J. Forsyth, “DC link current in PWM inverters with unbalanced and non-linear loads,” in *Proc. Inst. Elect. Eng. Electrical Power Applications*, Nov. 1999, vol. 146, no. 6, pp. 620–626.

[15]. P. Enjeti and S. Kim, “A new DC-side active filter for inverter power supplies compensates for unbalanced and nonlinear loads,” in *Proc. IEEE Industry Applications Society Annual Meeting*, 1991, vol. 1, pp.1023–1031.

[16]. Koilada Rajesh, “Novel Control of Boost Converter for MPPT of Wind Turbine”, International Journal of New Technologies in Science and Engineering (IJNTSE), Vol. 8, Issue. 6, pp. 1-6, June. 2022.

[17]. Kandi Bhanu Prakash, "PV-Battery based standalone power supply system for rural applications", International Journal of New Technologies in Science and Engineering (IJNTSE), Vol. 8, Issue. 12, pp. 9-13, Dec. 2022.